JOURNAL OF VIROLOGY, Nov. 1997, p. 8678–8689 Vol. 71, No. 11
0022-538X/97/$04.00+0

Structural and Functional Determinants in Adenovirus Type 2 Penton Base Recombinant Protein

LUCIE KARAYAN, SAW SEE HONG, BERNARD GAY, JEANNETTE TOURNIER, ARNAUD DUPUY D'ANGEAC, AND PIERRE BOULANGER*

Laboratoire de Virologie et Pathogénèse Moléculaires, Centre National de la Recherche Scientifique URA-1487, Faculté de Médecine, Montpellier, 34060 France

Received 24 April 1997/Accepted 12 August 1997

Discrete domains involved in structural and functional properties of adenovirus type 2 (Ad2) penton base were investigated with site-directed mutagenesis of the recombinant protein expressed in baculovirus-infected cells. Seventeen substitution mutants were generated and phenotyped for various functions in insect and human cells as follows. (i) Pentamerization of the penton base protein was found to be dependent on three amino acid side chains, the indole ring of Trp119, the hydroxylic group of Tyr553, and the basic group of Lys556. (ii) Arg254, Cys432, and Trp439, the stretch of basic residues at positions 547 to 556, and Arg340 of the RGD motif played a critical role in stable fiber-penton base interactions in vivo. (iii) Nuclear localization of penton base in Sf9 cells was negatively affected in mutants W119H or W165H, and, to a lesser extent, by substitutions in the consensus polybasic signal at positions 547 to 549. (iv) Penton base mutants were also assayed for HeLa cell binding, cell detachment, plasmid DNA internalization, and Ad-mediated gene delivery. The results obtained suggested that the previously identified integrin-binding motifs RGD^{340} and LDV^{287} were functionally and/or topologically related to other discrete regions which include Trp119, Trp165, Cys246, Cys432, and Trp439, all of which were involved in penton base-cell surface recognition, endocytosis, and postendocytotic steps of the virus life cycle.

The human adenoviruses (Ad) comprise a group of more than 40 serologically distinct viruses, but they have the same basic virus structure, namely, an icosahedral protein capsid with projecting fibers. The fibers are linked to a capsid anchorage domain, the penton base capsomer (38, 46). Ad fiber and penton base are both oligomeric proteins, fiber occurring as a trimer in its native conformation (54) and penton base occurring as a pentamer (7, 8, 53, 58). The penton capsomer is thus a heteromeric association of a pentameric base and a trimeric fiber (reviewed in reference 11). The penton base protein sequence is highly conserved between Ad of the same subgroup; 98.6% homology has been found between Ad2 and Ad5 (39), and chimeric penton capsomers, made of Ad2 base and Ad5 fiber, have been isolated in vitro and in vivo (6, 16). The features common to the penton bases of all human Ad subgroups and even to those of avian Ad (52) are two moieties of high homology separated by a nonhomologous spacer region of variable length which includes the conserved RGD motif (^{340}RGD in Ad2 [13, 34]). The conserved N-terminal domain comprises about 300 residues and includes the fiber binding site (^{254}RLSNLLG in Ad2 [24]).

The Ad particles enter their susceptible host cells by receptor-mediated endocytosis, and it is well established that the fiber and penton capsomers are responsible for the attachment of the virus to the cell surface (15, 31, 42, 51, 59). For Ad serotypes belonging to subgroup C (e.g., Ad2 and Ad5), the widely accepted mechanism for early steps in infection, i.e., attachment and entry, is a two-step model (37, 60) in which (i) cell attachment of Ad occurs via the distal portion of the fiber (the knob) to primary receptor(s), two of which have recently been identified (5, 25, 57), followed by (ii) the interaction of the five RGD motifs in the penton base capsomer with $\alpha_v\beta_3$ integrins identified as the secondary receptors, resulting in the endocytosis of the virion (4, 62, 63). Within the endosomal vesicle, the virions undergo a stepwise dismantling process which has been well documented (22). Cell membrane permeabilization and vesicular escape of the virion are thought to result from the selective interaction of adenovirus penton base with $\alpha_v\beta_5$ integrins (62).

With the exception of the conserved RGD motif (3, 4, 13, 34) and the fiber-binding site (24), no discrete regions or amino acid residues of the penton base have been assigned specific biological functions, such as those involved in endosomal escape of the virions (49, 50, 62). No conditionally defective mutants of Ad (e.g., temperature sensitive) have been isolated in the penton base gene (20, 33), suggesting that mutations in the penton base capsomer were detrimental to virus viability. These lethal effects could affect early functions of the virus life cycle, e.g., virus entry and capsid uncoating within the endosome or late stages of virion assembly within the nucleus.

In order to analyze the biological functions of the Ad2 penton base and their specifying domains, we generated a panel of substitution mutants in the recombinant protein expressed in the baculovirus system (28). The properties of the mutant proteins were studied in *cis* in Sf9 and HeLa cells as well as in *trans* in the coinfection of HeLa cells with adenovirions. We found that pentamerization, nuclear localization, and assembly with fiber depended upon the integrity of a few amino acid residues, often located at a distance from each other in the penton base linear sequence. Functions involved in Ad capsid-cell membrane interactions and Ad-mediated gene transfer were found to be altered by mutations in the two integrin-binding motifs RGD^{340} and LDV^{287} and in other residues located in both conserved structural domains. Our study provided some clues to the role of penton base in early steps of the Ad life cycle which could be of interest concerning the efficient delivery of therapeutic genes to target cells.

* Corresponding author. Mailing address: Laboratoire de Virologie & Pathogénèse Moléculaires, Institut de Biologie, Faculté de Médecine, 34060 Montpellier Cedex, France. Phone: 33 4 67 60 57 38. Fax: 33 4 67 54 23 78. E-mail: pboulang@infobiogen.fr.

MATERIALS AND METHODS

Cells and viruses. Wild-type (WT) Ad2 and Ad5 and recombinant Ad5Luc3 (35) were all propagated in HeLa cell monolayers. Parental baculovirus BacPAK6 and recombinant Ac*M*NPV were propagated in *Spodoptera frugiperda* Sf9 cell monolayers (28, 32). Construction of intermediate vectors and recombinant baculoviruses expressing Ad2 WT full-length fiber (F2FL582), Ad2 WT full-length penton base (PbFL571), penton base amino-terminal deletion mutant At69, and carboxy-terminal deletion mutants Ct550 and Ct531 have been described previously (28, 40).

Penton base mutagenesis. The three single substitution mutants D288K, R340E, and R340G and the double mutant D288K-R340E (abbreviated $K^{288}R^{340}$) were generated by site-directed mutagenesis performed on Ad2 penton base gene subcloned into the pBluescript II KS(−) phagemid (Stratagene) by the single-stranded DNA method (30), with R408 as the helper phage (47). The Asp-to-Lys mutation at residue 288 (LDV motif) was generated with the 32-mer oligonucleotide 5′-GC CTG GTA GGC GTC CAC CTT CAA CAG TGC GGG-3′ (Eurogentec, Seraing, Belgium), reproducing, except for codon 288 (underlined), the noncoding strand of the penton base gene sequence between nucleotides 15031 and 15000 (45). The Arg-to-Glu substitution at position 340 in the RGD motif was generated with the 31-mer oligonucleotide 5′-GGC AAA GGT GTC GCC CTC AAT GGC ATG ATC G-3′ (noncoding strand sequence between nucleotides 15185 and 15155, with mutated codon underlined). The R340G mutant resulted from a mispairing event which accidentally occurred in bacteria during the construction of R340E. The double mutant $K^{288}R^{340}$, constructed in two steps, carried both D-to-K and R-to-E substitutions at positions 288 and 340, respectively. All the other point mutants were generated by in vitro mutagenesis performed by the PCR technique with two complementary mutagenic oligonucleotides (23) whose sequences and positions in the Ad2 penton base gene will be provided upon request. DNA sequencing of the mutants was performed by the dideoxyribonucleotide chain termination method (48) and the Sequenase kit version 2.0 (USB-Sequenase; Amersham).

Gel electrophoresis and immunoblotting. Sodium dodecyl sulfate (SDS)-denatured and native proteins were analyzed by polyacrylamide gel electrophoresis (PAGE), as previously described (28). Immunological quantification of proteins on blots was carried out with ^{125}I-labeled secondary antibody (750 to 3,000 Ci of antibody per mmol; 5 to 20 μCi of antibody per μg; Amersham) at 3 to 5 μCi/blot and autoradiography. Autoradiograms (Hyperfilm-βmax; Amersham) were scanned at 610 nm with an automatic densitometer system (REP-EDC; Helena Laboratories, Beaumont, Tex.). The three primary rabbit antibodies used were directed against (i) cesium chloride-purified Ad2 virions, (ii) electrophoretically purified recombinant native Ad2 fiber, and (iii) electrophoretically purified recombinant Ad2 penton base and were all laboratory made.

Penton capsomer assembly in vivo. Assembly of recombinant penton capsomer was assayed in vivo in insect cells (28). Sf9 cells were coinfected at equal multiplicities of infection (MOI) (5 PFU/cell) by two recombinants, one expressing recombinant penton base (WT or mutant) and the other expressing WT fiber F2FL582. Cells were harvested at 48 h postinfection, and cell lysates were analyzed by the fiber band migration shift assay in nondenaturing PAGE and by immunoblotting with antifiber antibodies as previously described (24, 28).

Cell-detaching effect. Cell detachment from solid support provoked by recombinant penton base was assayed as previously described (28) with some modifications. HeLa cell monolayers (10^5 cells per well), prelabeled for 24 h with [^{3}H]thymidine (40 μCi/ml), were incubated with recombinant penton (1 μg in 200 μl of culture medium) at 37°C for 1 h. Adherent and detached cells were separately collected, dissolved in 1 M NaOH, 1% SDS, 1 M urea, and ^{3}H-labeled DNA precipitated in 10% trichloroacetic acid on GF/C filters. The proportion of detached cells was determined by counting acid-precipitable radioactivity in a liquid scintillation spectrometer (Beckman LS-6500).

Cell binding and internalization of penton base. Aliquots of 1 μg of recombinant penton base isolated from insect cell culture fluids were incubated with 10^5 HeLa cell samples in 200 μl of serum-free culture medium for 1 h at 0°C. This corresponded to 2×10^{12} penton base molecules per 9×10^9 theoretical penton base receptors (63), i.e., a 220-fold excess. At the end of this incubation period, the cells were washed three times in phosphate-buffered saline (PBS) and cell-adsorbed penton base was quantitated by SDS-PAGE and immunoblotting, as described above. For endocytosis assay, cells were transferred to 37°C for 20 min, cooled to 0°C, washed three times with cold Tris-buffered saline (pH 8.0) containing 1 mM $CaCl_2$ (TBS-Ca), and incubated for 1 h at 0°C in 200 μl of TBS-Ca with subtilisin (2 mg/ml) to remove nonendocytosed penton base. After 1 h, cells spontaneously detached. Subtilisin was inactivated by phenylmethylsulfonyl fluoride (1 mM final concentration), and the cells were collected and rinsed three times in phenylmethylsulfonyl fluoride-containing TBS. The cell samples were analyzed for intracellular penton base, as described above. Alternatively, recombinant penton base was labeled with both [^{35}S]methionine and [^{35}S]cysteine (Tran^{35}S-label, ICN; 1,380 Ci/mmol) at 20 μCi/ml in methionine- and protein-free medium, as previously described (24). The specific radioactivity of the samples used was 50,000 to 65,000 cpm per μg of protein, and cell-bound or cell-endocytosed radioactivity was determined by SDS-PAGE and autoradiography.

HRP internalization. Aliquots (20 μl) of horseradish peroxidase (HRP) solution at 2 mg/ml in H_2O were mixed with 280 μl of PBS and incubated with HeLa cell monolayers (10^5 cells) at 0°C for 1 h. After three rinses with cold PBS, 300 μl of PBS containing (or not) 1 μg of recombinant penton base was added to the cell monolayers, and the cultures were transferred to 37°C for 1 h to allow endocytosis to occur. The cells were then rinsed five times with cold PBS, lysed in hypotonic alkaline buffer (10 mM Tris-HCl [pH 8.9]–1 mM EGTA–0.1 mM PMSF), and endocytotic vesicles were recovered by centrifugation at 10,000 × *g* for 15 min (15). The endosomal fraction was solubilized in TKM-T buffer (50 mM Tris-HCl [pH 7.4]–25 mM KCl–5 mM $MgCl_2$–0.5% Triton X-100) and assayed for endocytosed HRP (15).

Plasmid delivery. Plasmid-based expression vector carrying the firefly luciferase gene under the control of the simian virus 40 (SV40) late promoter was purchased from Promega (pGL3-control vector). The technique of transfection with cationic polymer polyethylenimine (PEI [9]) in the presence of recombinant penton base was derived from that described by Yoshimura et al. (68) for Ad particles, with some modifications. In standard experiments, 9 μl of PEI titrating 5.47 mM for nitrogen (ExGen500; Euromedex, Souffelweyersheim, France) was diluted to 50 μl in PBS and mixed with 50 μl of PBS containing 3 μg of pGL3. The final mixture (100 μl) was added to HeLa cell monolayers (10^5 cells per sample) overlaid with 300 μl of serum-free culture medium containing 1 μg of recombinant penton base preincubated with the cells at 0°C for 30 min. The cells were transferred to 37°C for 3 h, the supernatant was removed and replaced by prewarmed culture medium, and the cultures were further incubated at 37°C for 24 h and processed for luciferase assays. Luciferase activity, expressed as relative light units (RLU), was determined as previously described (25).

Ad-cell interactions and Ad-mediated gene transfer. [^{3}H]thymidine-labeled WT Ad5 virions (specific radioactivity of 10^6 cpm per 10^{11} virions) and recombinant Ad5Luc3 carrying the luciferase reporter gene were used.

(i) Ad-cell binding. This was assayed with HeLa cells at 0°C, a temperature which allows Ad binding to cell surface receptors but does not allow endocytosis (15, 44, 55, 56, 65). Aliquots of ^{3}H-labeled Ad5 in PBS (5×10^4 cpm per 10^5 cells) corresponding to 5×10^4 Ad5 per cell, i.e., more than fivefold the number of cell receptors (15, 42, 51), were mixed with a fixed amount of WT or mutant penton base (1 μg per 10^5 cells), and the mixture, cooled to 0°C, was added to HeLa cell monolayers maintained at 0°C. After incubation at 0°C for 1 h, unadsorbed virus was removed by rinsing with cold PBS, and the cells were resuspended and washed twice in cold PBS. The cell pellet was dissolved in a solution containing 1 M NaOH, 1% SDS, and 1 M urea for 1 h at 37°C, and acid-precipitable radioactivity was determined as described above. Ad5Luc3 at various MOI was mixed with constant amounts (1 μg per 10^5 cells) of penton base protein (WT or mutant), and the mixture, cooled to 0°C, was added to HeLa cell monolayers maintained at 0°C. After incubation at 0°C for 1 h, the cell samples were rinsed twice with cold culture medium to remove unadsorbed virus. The culture was then shifted to 37°C and further incubated for 16 h, and cells were processed for luciferase assay, as previously described (25). When luciferase activity of cell lysates was plotted versus Ad5Luc3 MOI, a linear relation of virus dose-luciferase response was obtained for MOI ranging from 0.02 to 0.25 PFU/10^5 cells (25). The results were expressed as the ratios (in percentages) of the slope of the plots obtained with WT or mutant penton base to the slope of the plot obtained with control cells infected with Ad5Luc3 in the absence of penton base.

(ii) Ad endocytosis and cell entry. [^{3}H]thymidine-labeled WT Ad5 virions were incubated with HeLa cells at the ratio of virus to cells used in the previously described assay for 1 h at 0°C. Unadsorbed virus was rinsed off with cold medium, and recombinant penton base (WT or mutant) was added at the time of temperature shift to 37°C, as described above. After 1 h at 37°C, the cells were rinsed once with TBS-Ca and incubated in 200 μl of TBS-Ca with subtilisin (2 mg/ml) for 15 min at 37°C to release the noninternalized virus. The cells were then pelleted, rinsed twice with TBS, and processed for radioactivity counting. When Ad5Luc3 was used, the cells were rinsed twice with medium, further incubated with fresh, prewarmed medium for 16 h, and then processed for luciferase assays. Control experiments for possible cellular toxicity of penton base mutants or side effects on luciferase expression in the two previously described assays consisted of preincubating HeLa cell monolayers with Ad5Luc3 for 1 h at 37°C, a temperature at which both cell attachment and entry occur. Unadsorbed virus was then rinsed off, penton base protein was added to the cells for 1 h at 37°C, and luciferase was assayed at 16 h. Luciferase activity was then corrected for possible negative cellular effects of penton base.

Cytology. Processing of cell specimens for conventional electron microscopy (EM) and for antibody-immunogold labeling and quantitative immunoelectron microscopy (IEM) has been described in detail elsewhere (10). Sections were examined under a Hitachi-H7100 electron microscope, and cell compartments were quantitatively analyzed for immunogold labeling by scanning EM photographs with an image analyzer (Agfa Arcus2-PCF) and the National Institutes of Health Image program, version 1.60. Cell viability was analyzed by flow cytometry, performed by differential cell labeling with Hoechst-33342 reagent and propidium iodide in a FACScan flow cytometer (Becton Dickinson, Mountain View, Calif.).

RESULTS

Rationale for site-directed mutagenesis of Ad2 penton base. A panel of 17 substitution mutants of the Ad2 penton base gene were constructed and expressed as recombinant proteins in the baculovirus expression system. All the mutations gener-

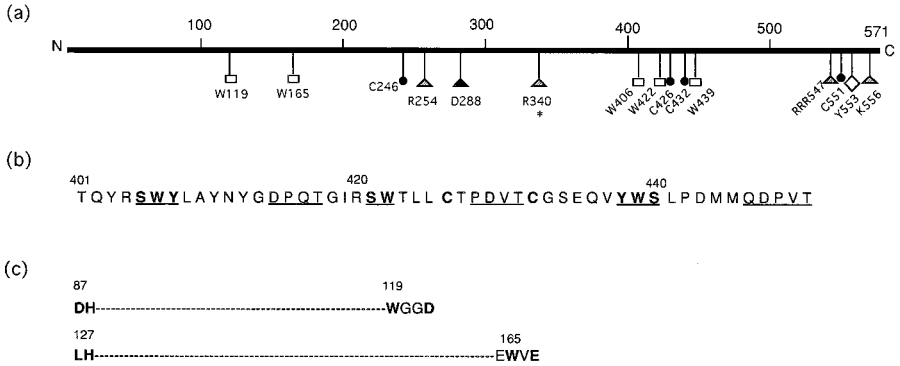

FIG. 1. (a) Linear representation of Ad2 penton base molecule showing the position of the different substitution mutants. (b) Amino acid sequence of the penton base protein within residues 401 to 450 showing the inverted tripeptide repeats SWY/YWS (underlined and bold-faced) and the DPQT/QDPVT repeated motifs (underlined). The two cysteine residues are bold-faced. (c) Amino acid sequence of the penton base protein within residues 87 to 199 and 127 to 165, showing the homology with GH (30 residues)-WD repeats (36).

ated were nonconservative in terms of residue side chain and potential interactions but conservative with respect to hydrophilicity and hydrophobicity and probability of secondary structure of the mutant protein domains as follows. (i) The cysteine residues at positions 246, 426, 432, and 551, which were not involved in intermonomer disulfide bonds in penton capsomers (7, 43) but could theoretically form intrachain bonds, were substituted for serine (Fig. 1a). (ii) The indole ring of the five tryptophan residues was replaced by the imidazole ring of histidine, generating mutants W119H, W165H, W406H, W422H, and W439H. In protein-protein interactions, indole rings of tryptophan side chains contribute to the free energy of binding because of their large surface areas and because they have relatively low conformational entropy, resulting in a lower entropy change when they become immobilized in the interface (14). In the Ad2 penton base sequence, the tryptophan residues present some pattern of symmetry. For example, the SW dipeptide is found twice at positions 405 and 421 and a third time in the reverse orientation (WS) at position 439. Even more striking, the SW motif at 421, followed by two cysteine residues (Cys426 and Cys432), is flanked by the motif SWY at 405 and its reverse-oriented tripeptide YWS at 438 (Fig. 1b; refer to the penton base sequence in reference 39). At the N-terminal moiety of penton base, it is noteworthy that the motifs WGGD and WVE, at positions 119 and 165, respectively, are located 31 and 37 residues downstream from the dipeptides DH at position 87 and LH at position 127 (Fig. 1c). This is reminiscent of the WD repeat protein family, whose members have been reported to possess functions in cell trafficking or control of gene expression (36). (iii) Two major cell adhesion motifs have been identified in Ad2 penton base (4), the integrin ligand RGD motif (27, 66) at position 340, and the core peptide LDV at position 287. RGD is highly conserved in the penton base in all Ad serotypes sequenced thus far (13, 34) and has been shown to play a role in the recognition of penton base by integrins $\alpha_v\beta_3$, $\alpha_v\beta_5$, and $\alpha_M\beta_2$ (2, 3, 37, 61–64). LDV has been shown to specifically interact with integrins $\alpha_4\beta_1$ and $\alpha_4\beta_7$, expressed mainly on lymphocytes, monocytes, and fibroblasts (29, 61). Three mutants were constructed in these two regions, D288K, R340E, and R340G, together with the double mutant D288K+R340E, referred to as $K^{288}E^{340}$. (iv) At the fiber-binding site (^{254}RLSNLLG^{260} [24]), the basic residue arginine was changed to glutamic acid, generating the R254E mutant. (v) Three mutants were also generated within the basic carboxy-terminal region, which has been found to be critical for pentamer structure (28) and contains a potential nuclear localization signal: Tyr553 was changed to the highly conserved aromatic residue Phe (Y553F), and a stretch of basic residues (^{546}ARRRTCPYVYKA^{557}) was substituted for acidic and/or neutral residues, giving rise to the triple substitution mutant RRR^{547}EQQ, and a single point mutant, K556E. Carboxy-terminal deletion mutants Ct550 and Ct531 and amino-terminal deletion mutant At69, previously published (28), have also been included in this study.

Expression of recombinant penton base mutants in baculovirus-infected cells. None of the mutations created was found to be deleterious to the expression of the recombinant penton base in Sf9 cells, and all the mutants were expressed at levels comparable to that of the WT clone PbFL571 (Fig. 2a). As for WT penton base in human cells (19), no apparent cytotoxic effect was observed in insect cells. This was also analyzed by flow cytometry, which showed no influence of recombinant penton base protein on HeLa cell viability (data not shown). All the penton base mutants were secreted at high levels in Sf9 culture medium, with the exception of the low secreter mutant W165H (data not shown). The recombinant penton base mutants were then phenotyped according to the following biological functions in *cis*: (i) pentamerization, (ii) assembly with fiber and penton capsomer formation, (iii) cellular localization in recombinant baculovirus-infected Sf9 cells, (iv) cell-detaching effect, (v) attachment to HeLa cell surface and endocytosis, (vi) cointernalization of HRP, (vii) penton base-mediated plasmid-borne gene delivery, and (viii) Ad-mediated gene delivery. The effects of the mutants were also analyzed in *trans* in HeLa cells, in competition with adenovirions for cellular attachment, endocytosis, and endosomal escape.

Pentamerization. Ad2 penton base naturally occurs as a homopentameric protein of 571 amino acid residues (43). Recombinant Ad2 WT PbFL571 expressed in insect cells has been found to self-assemble into penton base capsomers (9S pentamers) with a high efficiency, whereas the carboxy-terminal deletion mutants Ct550 and Ct531 fail to pentamerize (28), suggesting that the integrity of the carboxy-terminal 21 residues of the penton base sequence is essential for pentamerization. Pentamerization of penton base mutants was assayed in nondenaturing gels, where monomers migrate as a diffuse band at the position of the serum albumin marker, whereas pentamers appear as a discrete band with slower electrophoretic mobility (28). All of the four cysteine mutants retained their capacity to pentamerize (Fig. 2b), although C551S and C432S pentamerized with a lower efficiency (Table 1). This pattern implied that disulfide bonds were not directly (via interchain bonds) or

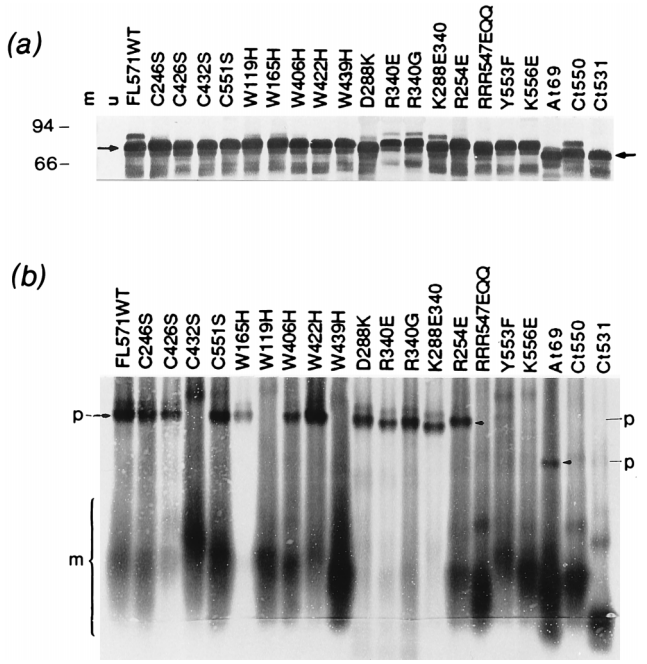

FIG. 2. Expression of recombinant penton base in baculovirus-infected Sf9 cells. (a) SDS-PAGE analysis of whole-cell lysates showing the level of expression of WT (FL571WT) and mutant polypeptides. m, prestained molecular mass markers; u, mock-infected cell extracts. On the left are molecular mass markers for phosphorylase (94 kDa) and bovine serum albumin (66 kDa). Shown is a blot reacted with anti-penton base rabbit antibody and phosphatase-conjugated secondary antibody. Arrows indicate the position of recombinant penton base polypeptide. (b) Immunoblot of WT- and mutant-expressing whole-cell lysates electrophoresed under native conditions. m, penton base monomers migrating as a diffuse zone; p, the discrete band of pentamers. Note the difference in electrophoretic migration between some mutants due to the difference in their net electric charges.

indirectly (via intrachain bonds) involved in the pentamerization process. Two mutants in the N-terminal moiety of the protein were found to be partially (R254E) or totally (W119H) defective in pentamerization. Within the C-terminal domain, mutants W439H, $RRR^{547}EQQ$, Y553F, and K556E also showed pentamerization-defective phenotypes (Fig. 2b and Table 1). This suggested that the hydroxylic group of Tyr553, the indole ring of Trp119 and Trp439, and the stretch of basic residues at positions 547 to 556 were essential for the formation and/or maintainance of the pentameric structure of the penton base capsomer.

Interaction with fiber and assembly into penton capsomer in vivo. Recombinant Ad2 WT penton base PbFL571 and fiber F2FL582 have been shown to be capable of assembling into penton capsomers when coexpressed in *trans* within the same insect cell (28). Each penton base mutant was thus tested for its capacity to reconstitute penton capsomers in vivo upon coexpression with recombinant fiber F2FL582, as assayed by the occurrence of a discrete band of slower-migrating penton capsomer in native PAGE and immunodetection with antifiber antibody (Fig. 3a). Several mutants located in the C-terminal domain, C432S, W439H, $RRR^{547}EQQ$, and K556E, and the two deletion mutants Ct550 and Ct531 failed to assemble into penton, but two mutants in the same domain, C551S and Y553F, still interacted with fiber. Penton capsomer assembly was significantly reduced, although not totally abolished, for W119H, W165H, R254E, R340E, and W406H (Fig. 3a and Table 1). These results suggested that, besides the fiber-binding site (24), several other discrete regions played a role in penton base fiber-specific interactions and/or the stability of the bonds; one involved residues 432 to 439, and the other involved the polybasic signal at positions 547 to 556. The somewhat unexpected difference between R340E (penton defective) and R340G (WT phenotype) also implied an important role for the basic charge of the RGD adhesion motif in penton capsomer stability. There was no apparent correlation between the deficiency in the pentamerization of the penton base mutant proteins and their defect in assembly with fiber in insect cells; K556E and $RRR^{547}EQQ$ occurred mainly as monomers and failed to assemble with fiber, but monomers of W119H and Y553F were still capable of a significant level of assembly with fiber.

Cellular localization in insect cells. The nuclear localization of our penton base mutants was studied by IEM, and the cellular distribution of anti-penton base gold grains was estimated by scanning and counting IEM photographs (10, 40). The results are summarized in Table 1. There was no correlation between the nuclear localization pattern and pentamerization of the penton base. Recombinant WT penton base PbFL571 distributed almost proportionately between the nucleus (N) and cytoplasm (C) of Sf9 cells (Fig. 4a), with an N:C ratio of 1.30. Mutants R254E, C426S, C432S, C551S, D288K, K556E, and W422H showed a WT pattern (ratio, 1.0 to 1.8), whereas mutants R340E and W439H showed an apparent enhancement of nuclear transport, with ratios of 5.7 and 2.9, respectively. Mutations C246S, $K^{288}E^{340}$, W406H, and $RRR^{547}EQQ$ significantly lowered the nuclear transport of penton base, with an N:C ratio of 0.4 to 0.7, but the most deleterious effect was obtained with two mutations, W119H (Fig. 4b) and W165H, with an N:C ratio of 0.1 (Table 1). This observation excluded the possibility of a unique nuclear localization signal in penton base and suggested that regions overlapping Trp119 and Trp165 contained a nonclassical nuclear localization signal (1, 21) in addition to the consensus polybasic signal at positions 546 to 556 near the C terminus.

Cell-detaching effect. The conserved RGD and LDV motifs found in penton base are characteristic of cell adhesion proteins. Mutation in the RGD core peptide of Ad2 penton base capsomers has been shown to modify its cell-detaching activity (3). As expected, our RGD mutant R340E was eight times less efficient than WT penton base in provoking HeLa cell detachment. The same reduced effect of cell detachment was observed for the LDV motif mutant D288K and for W165H and C246S (Table 1). This strongly suggested that residues Trp165 and Cys246 belonged to the same functional domain(s) as Asp288 and Arg340, acting by competition with extracellular cell adhesion molecules. For the double mutant $K^{288}E^{340}$, however, cell detachment activity was reduced by only twofold compared to that for WT. This implied a certain degree of complementation between the two mutations with opposite electric charges, R-to-E^{340} and D-to-K^{288}, when carried in *cis* by the same protein. Previous studies on the binding of penton base to $\alpha_v\beta_3$ and $\alpha_v\beta_5$ integrins have shown that binding to $\alpha_v\beta_3$ was RGD dependent, while binding to $\alpha_v\beta_5$ occurred in an RGD-independent manner (62, 63). The following experiments were designed to verify whether residues in penton base other than the ones present in the RGD and LDV core peptides could account for penton base binding to the cell surface.

Penton base attachment and endocytosis by HeLa cells. Epithelial, hematopoietic, and fibroblastic cells have been found to be able to internalize penton base provided they express $\alpha_v\beta_3$, $\alpha_v\beta_5$, $\alpha_M\beta_2$, $\alpha_4\beta_1$, or $\alpha_4\beta_7$ integrins at their surfaces (26, 61–64). Recombinant penton base carrying mutations in the integrin-binding motifs R340E, R340G, and D288K and the

TABLE 1. Effects of mutations in *cis* on phenotypes of penton base

Mutant or control	Ratio of pentamers/monomers[a]	Assembly with fiber[b]	Nuclear localization[c]	Cell-detaching titer[d]	HRP endocytosis[e]	Plasmid delivery[f]
Control					323 ± 80 (1.0)	1.00
FL571WT	95.8:4.2	100.0	1.30 ± 0.54	66	510 ± 150 (1.6)	2.47 ± 0.10
C246S	87.5:12.3	40.6	0.57 ± 0.09	19	593 ± 430 (1.8)	1.55 ± 0.30
C426S	96.3:2.7	62.5	0.93 ± 0.19	44	826 ± 390 (2.5)	2.18 ± 0.50
C432S	49.2:50.5	0.0	1.81 ± 1.22	32	719 ± 400 (2.2)	2.93 ± 0.28
C551S	78.9:21.1	55.6	1.23 ± 0.26	43	759 ± 150 (2.3)	2.82 ± 0.15
W119H	11.9:88.0	17.5	0.13 ± 0.02	40	634 ± 330 (2.0)	3.24 ± 0.27
W165H	100.0:0.0	23.7	0.12 ± 0.04	12	635 ± 490 (2.0)	0.92 ± 0.17
W406H	89.0:10.8	22.5	0.42 ± 0.19	33	453 ± 100 (1.4)	1.81 ± 0.36
W422H	85.1:14.9	72.0	1.49 ± 0.18	39	930 ± 530 (2.9)	0.91 ± 0.12
W439H	33.2:65.1	0.0	2.87 ± 2.13	32	438 ± 210 (1.4)	1.45 ± 0.28
D288K	98.8:0.9	42.5	1.04 ± 0.14	7	500 ± 400 (1.5)	1.07 ± 0.29
R340E	100.0:0.0	7.5	5.69 ± 0.54	8	405 ± 300 (1.2)	0.80 ± 0.22
R340G	100.0:0.0	64.4	ND[g]	28	662 ± 340 (2.0)	1.56 ± 0.20
$K^{288}E^{340}$	100.0:0.0	40.6	0.68 ± 0.16	27	565 ± 410 (1.7)	1.55 ± 0.26
R254E	52.7:46.9	11.2	1.44 ± 0.13	62	354 ± 110 (1.1)	2.16 ± 0.16
$RRR^{547}EQQ$	20.4:79.1	0.0	0.55 ± 0.29	36	395 ± 170 (1.2)	2.26 ± 0.10
Y553F	17.9:81.9	24.4	0.98 ± 0.19	47	851 ± 430 (2.6)	2.08 ± 0.20
K556E	11.7:87.9	0.0	0.94 ± 0.30	61	832 ± 360 (2.5)	1.90 ± 0.57
At69	13.6:86.3	18.5	ND	55	419 ± 190 (1.3)	2.33 ± 0.39
Ct550	14.7:83.2	0.0	ND	48	452 ± 140 (1.4)	2.70 ± 0.46
Ct531	5.8:92.8	0.0	ND	32	387 ± 100 (1.2)	2.13 ± 0.15

[a] Ratio of pentamers to monomers in native gels (refer to Fig. 2b). Results represent the mean (M) of four separate experiments ($n = 4$). Standard deviations (SDs) were within 15% of M values.

[b] Based on the occurrence of penton capsomer band in native PAGE of Sf9 cells coexpressing WT fiber and penton base, as shown in Fig. 3a. Results are expressed as percentages of WT. SDs were within 15% of M values ($n = 3$).

[c] Results (M ± SD, $n = 4$) are given as the ratio of intranuclear to intracytoplasmic density of immunogold grains (expressed as number of grains/μm^2), determined on at least four different fields in separate IEM photographs. Over 2,000 grains were counted (Fig. 4).

[d] Cell-detaching titer corresponded to the quantity of radioactively labeled HeLa cells detached from the solid support after incubation with penton base at 5 μg/ml at 37°C for 1 h. Results are the Ms of three separate experiments. SDs were within 20% of M values.

[e] HRP activity minus endogenous peroxidase activity is expressed as milliunits of enzyme activity per microgram of cell protein (M ± SD, $n = 4$). Values in parentheses are percentages of control, i.e., spontaneous cellular HRP uptake occurring in the absence of recombinant penton base.

[f] Plasmid-based expression vector carrying the luciferase gene was transfected to HeLa cells with PEI (9) in the absence (control) or presence of WT or mutant penton base. The results (M ± SD, $n = 4$) of luciferase activity in cell lysates are given as the ratio to that in control samples. The absolute M value for luciferase activity in control samples was 3.5×10^7 RLU/mg of cell protein.

[g] ND, not determined.

double mutant $K^{288}E^{340}$ bound to HeLa cells with a reduced efficiency. Mutant W165H also bound poorly to the cells, a phenotype which was consistent with its low cell-detaching effect. W406H, W422H, W439H, and Ct531 also bound to the cells in significantly lower amounts than WT and showed a lower cell-detaching activity (Fig. 5a and b and Table 1). For some mutants, however, there was an apparent discrepancy between cell-binding phenotype and cell-detaching effect. For example, C551S and Y553F, which bound to HeLa cells at WT or even higher levels, showed a lower cell detachment capacity. On the other hand, mutant K556E, which showed a WT phenotype for cell detachment, was defective for cell binding (Fig. 5a and b and Table 1). This suggested that motifs other than the consensus integrin-binding peptides and plasma membrane molecules different from the previously identified integrins could serve as penton base receptors.

To determine whether these putative cell surface molecules represented specific penton base receptors with a biological function in the viral cycle ("functional receptors"), each individual mutant was assayed in cell-binding competition with WT PbFL571. As shown in Fig. 5c, only 50 to 55% of WT penton base could be displaced by itself, implying that almost half the bound protein remained irreversibly adsorbed to the HeLa cell surface. When added to HeLa cells in a 30-fold excess over PbFL571, the group of mutants in the cell adhesion motifs, D288K, R340E, R340G, and $K^{288}E^{340}$, as well as W165H and Ct531 competed poorly with WT penton base, implying that they were all altered in specific receptor binding domains. The other mutants showed similar levels of competition with WT penton base, including the high-efficiency binding mutants C551S, Y553F, and At69. This suggested that their high level of cell binding represented adsorption to a significant proportion of nonspecific receptor(s).

Upon binding to the cell surface, penton base has been found to be rapidly endocytosed (62, 63). We therefore compared the efficiency of endocytosis of WT and penton base mutants. The endocytosis pattern resembled that of the cell surface attachment. For example, the integrin-binding mutants D288K, R340E, R340G, and $K^{288}E^{340}$ and W165H and Ct531, which were all defective for cell binding, were also internalized with a low efficiency (data not shown). Mutant C551S, however, which bound to the cells with a higher efficiency than WT

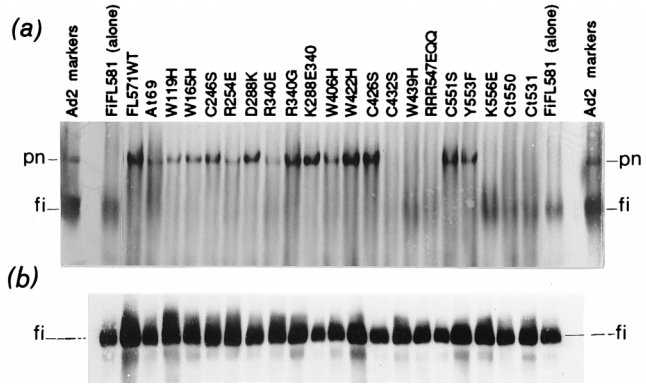

FIG. 3. Assembly of penton capsomer in vivo, in Sf9 cells coexpressing WT fiber and WT or mutant penton base, as indicated above the lanes. Note that the penton base mutants are presented differently from those in Fig. 1 and 2 and Tables 1 and 2; they are sequentially arranged from the N terminus on the left toward the C terminus on the right. Cell lysates were analyzed by PAGE under native conditions (a) or SDS-PAGE (b) and by immunoblotting. Blots were reacted with anti-fiber rabbit antibody and ^{125}I-labeled anti-rabbit immunoglobulin G secondary antibody (3 μCi/blot). Shown are autoradiograms of the blots. (a) Native samples, showing the diffuse band of fiber (fi) and the discrete band of assembled penton capsomer (pn). Ad2 capsid protein markers, fiber, and penton capsomers are on both sides. (b) SDS-denatured protein pattern of whole-cell lysates showing that recombinant fiber was expressed in similar amounts in all coinfected cells. The apparently inconsistent content of fiber in the different samples shown in panel a was therefore due to the effects of some penton base mutants on the solubility of coexpressed fiber, as previously observed (28).

(Fig. 5 a and b), was found to be internalized at WT levels. These results confirmed that the integrin pathway represented the most efficient endocytotic route for penton base and that penton base receptors other than integrins corresponded to nonspecific binding sites, which were nonfunctional in terms of the postattachment steps of the virus life cycle.

Effect of penton base on HRP internalization by HeLa cells. Cell permeability to a variety of macromolecules has been found to be enhanced during the course of Ad infection (41, 50, 67). In a previous study, we showed that the endocytosis of HRP, which normally accumulates within the lysosome compartment, was augmented twofold in HeLa cells by intact Ad2 or Ad5 virions (15). We therefore addressed the question of whether recombinant penton base (WT and mutants) was capable of reproducing the phenomenon observed with virions. WT penton base PbFL571 induced a 1.6-fold increase in HeLa cell endocytosis of HRP, a level comparable to that observed with Ad2 virions. Several mutations localized in the carboxy-terminal domain had a positive effect: a 2.9-fold increase was obtained with W422H; a 2.5-fold increase was obtained with C426S, Y553F, and K556E; and a 2.2-fold increase was obtained with C432S and C551S. Other mutants, R254E, RRR^{547}EQQ, and Ct531, had no significant effect on HRP cellular uptake, which remained at control levels (Table 1). Among the integrin-binding mutants, only R340E was defective in HRP endocytosis enhancement, whereas D288K, K^{288}E^{340}, and R340G showed a similar or higher effect than the WT (Table 1). This suggested that penton base-mediated enhancement of HRP internalization did not consist of a simple coendocytosis of two types of protein molecules depending on the RGD^{340} and LDV^{287} motifs and the integrin-binding pathway but depended also on alternative pathway(s) involving different domains in penton base. These domains could include residues within the 422 to 432 and 551 to 556 regions.

The enhancement in HRP internalization was relatively low (Table 1 and reference 15) compared to the 10-fold increase observed with the firefly luciferase (41) or the 100- to 10,000-fold increase observed with a bacterial toxin (18) in the presence of Ad virions. This could be due to the high rate of binding and internalization of HRP spontaneously occurring in the absence of virus or penton base. On the other hand, in the latter studies, researchers investigated both adenovirion-induced endocytosis and vesicular escape, whereas with our HRP assay we essentially explored the single endocytotic step. Similar results were obtained with firefly luciferase in the same type of assay (data not shown), suggesting that the observed effects of penton base on the endocytosis of macromolecules were not restricted to HRP.

Penton base and plasmid vector delivery to HeLa cells. The efficiency of gene delivery of a liposome-encapsulated expression vector is significantly enhanced in the presence of Ad particles (12, 68). To examine the possible contribution of penton base in this facilitation, we analyzed the effect of WT and mutants on the efficiency of transfection of HeLa cells with PEI-complexed plasmid-borne luciferase gene. In the presence of WT penton base PbFL571, luciferase activity increased by a factor of about 2.5, compared to the vector alone (Table 1). The Ad-mediated augmentation of plasmid delivery was therefore due to a certain extent to the penton base capsomers, but our results clearly indicated that free penton base does not possess the DNA delivery activity of the whole virion. An Ad-mediated 10,000-fold enhancement of DNA delivery was originally found with polylysine (12), and the value of our enhancing factor obtained with PEI was also significantly lower than the range of values (4- to 100-fold) recently reported for Ad augmentation of cell transformation with cationic liposomes (68). However, our enhancing factor was of the same order of magnitude as the one obtained with Ad3 penton dodecamers and DOTAP (17). With four mutants, D288K, R340E, W165H, and W422H, the luciferase activity remained at control levels, and with four others, R340G, K^{288}E^{340}, C246S, and W439H, the effect was significantly lower than WT. All these mutants were defective in integrin-binding and/or had a low cell-detaching effect (Table 1). This implied that penton base-mediated facilitation of PEI-complexed DNA delivery occurred mainly via the integrin pathway and integrin-binding motifs in penton base. However, other sequences might be involved, as certain mutations (W119H, C432S, and C551S) had a positive effect on plasmid delivery facilitation.

Role of penton base at early stages of Ad-HeLa cell interactions. Previous studies have shown that 10 to 25% of Ad virions bind irreversibly to cell surface molecules (4, 63). Similarly, our binding competition data (Fig. 5c) suggested that two types of penton base receptors coexist at the cell surface: specific receptors, identified as integrin molecules, which lead to virus uncoating, nuclear import, and virus replication; and nonspecific receptors, which represent a biological dead end for the virus. Furthermore, common cell adhesion sequences are found in fiber and penton base; the LDV motif exists at position 268 in the Ad2 fiber shaft, and an RGD-like motif is found as the antisense peptide SDGK at position 153 (43). SDGK is highly homologous to the SDGR peptide, which competes the most efficiently with Ad2 cell attachment (4). Penton base might thus theoretically interfere with Ad binding to both fiber and penton base receptors.

The effects of penton base mutants on early steps of Ad infection were analyzed by incubating HeLa cells with Ad particles in the presence of recombinant penton base added in large excess over Ad receptors. We used both recombinant Ad5Luc3 and [^{3}H]thymidine-labeled Ad5. In cell-binding assays performed at 0°C, cell-bound [^{3}H]Ad5 explored both specific and nonspecific receptors, whereas Ad5Luc3 luciferase

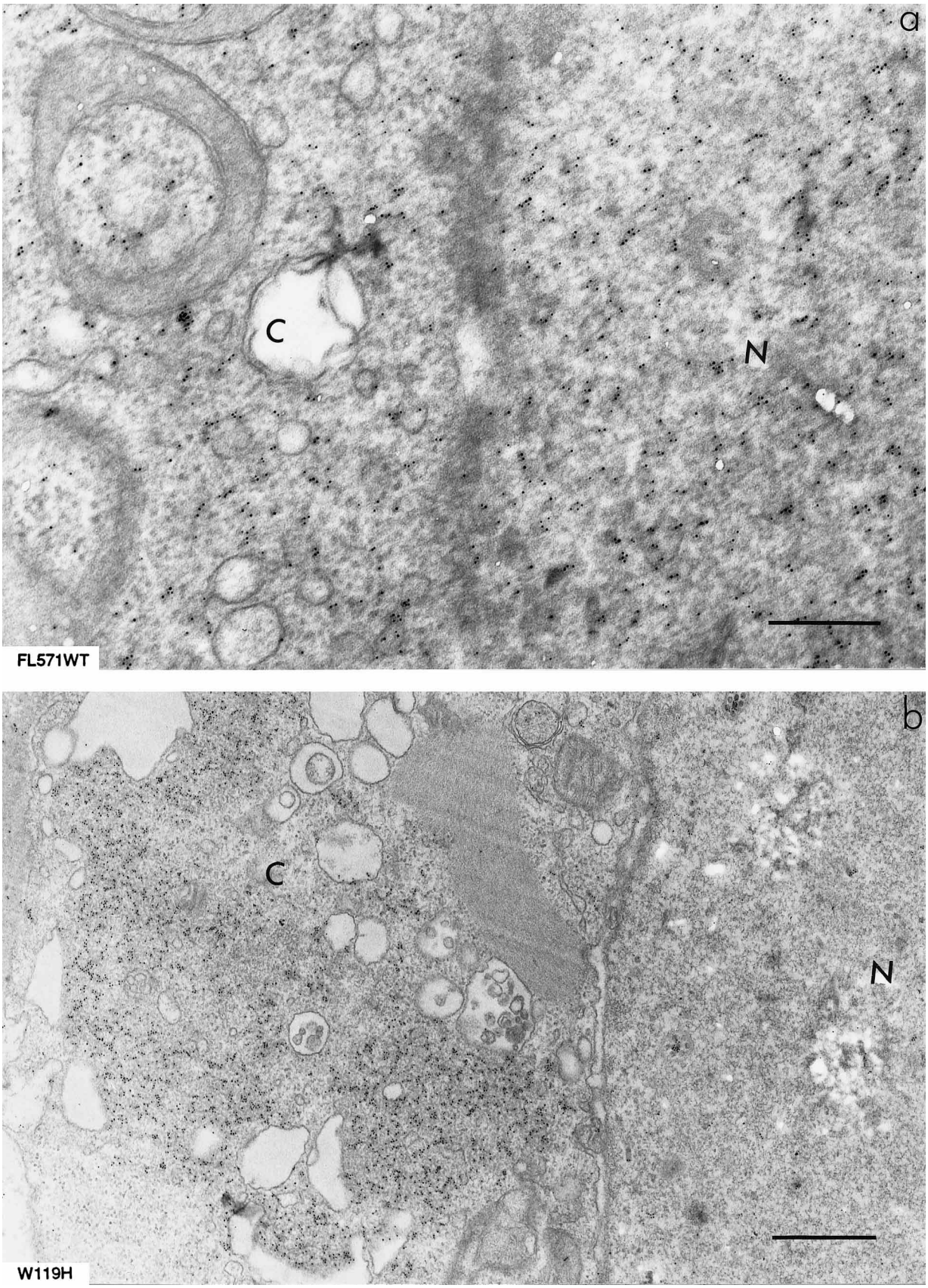

FIG. 4. IEM of Sf9 cell infected with (a) WT recombinant penton base (FL571) and (b) W119H mutant at 40 h postinfection. Cell sections were reacted with rabbit anti-penton base primary antibody and 5-nm gold-labeled anti-rabbit immunoglobulin G secondary antibody. N, nucleus; C, cytoplasm. Bar, 200 nm (a) and 300 nm (b).

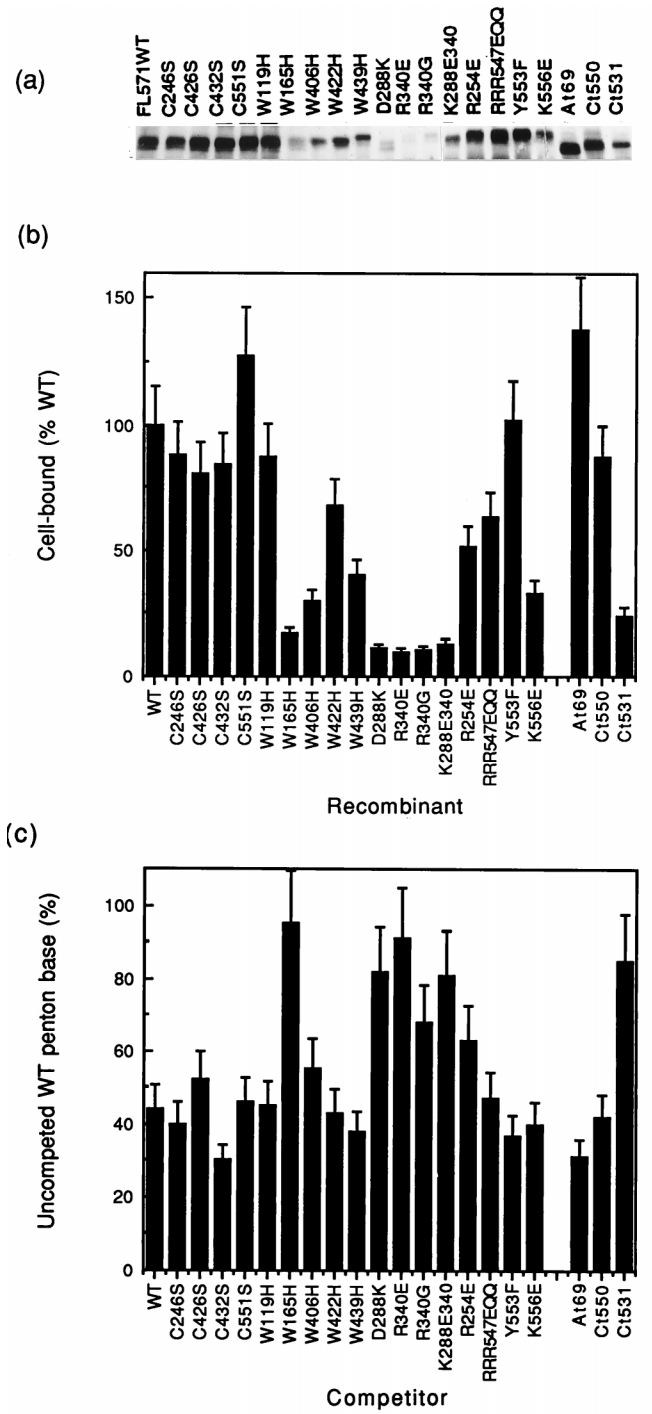

FIG. 5. Cell-binding of penton base mutants. The efficiency of penton base attachment to HeLa cell monolayers at 0°C was analyzed by SDS-PAGE and immunoblotting with anti-penton base rabbit antibody. (a) Autoradiogram of immunoblot obtained with ^{125}I-labeled anti-rabbit immunoglobulin G antibody (5 μCi/blot). (b) Quantification of cell-bound penton base performed by scanning of autoradiograms as shown in panel a. Values in the histogram represented the average of six different experiments. (c) Competition between WT and mutants. Aliquots (1 μg of protein) of ^{35}S-labeled FL571WT penton base (60,000 cpm/μg) were mixed with a 30-fold excess of unlabeled penton base mutant and incubated with HeLa cells at 0°C for 1 h. Uncompeted, irreversibly cell-bound WT penton base was determined by SDS-PAGE, autoradiography, and scanning of the penton base band on the autoradiogram. Note the low competing capacities of mutants W165H, D288K, R340E, $K^{288}E^{340}$, and Ct531.

expression probed for specific Ad receptors, since the luciferase activity resulted from the fraction of cell-bound virus which had effectively been endocytosed, released from the endosomal compartment, transported to the nucleus, and transcribed. Thus, the ratio of luciferase activity to ^{3}H radioactivity represented the usage of specific versus nonspecific receptors by the virus. Likewise, in endocytosis assays conducted at 37°C, the level of Ad5Luc3 luciferase expression, compared to the amount of cell-associated [^{3}H]Ad5, reflected the efficiency of endocytosis and postendosomal steps.

(i) Penton base interference with Ad attachment at 0°C. WT penton base PbFL571 showed no significant effect on the overall cellular binding of [^{3}H]Ad5 and only a slight inhibition (about 10% of the control samples) of Ad5Luc3 attachment (Fig. 6a and Table 2). Although this inhibition could be due to steric hindrance by the penton base, it could also mean that 10% of Ad particles bind to the cells via penton base receptors. In this case, soluble WT penton base would compete with intact Ad for both specific and nonspecific penton base receptors, whereas integrin-binding mutants would mainly compete for nonspecific receptors, effectively resulting in more virions available to specific receptors. As expected (Table 2 and Fig. 6a), mutants D288K and R340E as well as W165H, C246S, C432S, and W439H induced an apparent enhancement of Ad cellular binding, suggesting that the amino acids involved, Asp288, Arg340, Trp165, Cys246, Cys432, and Trp439, were functionally related.

(ii) Ad endocytosis and Ad-mediated gene delivery. In this assay, penton base could only interfere at the postattachment step and at the secondary receptor level, since Ad5 virions were preadsorbed at 0°C onto HeLa cells before the cell culture was transferred to 37°C in the presence (or absence) of the recombinant protein. WT PbFL571 had a more pronounced negative effect (about 30% inhibition) on Ad5Luc3 luciferase gene expression than on [^{3}H]Ad5 cellular uptake (less than 10%), with a value of 0.75 for gene delivery efficiency (Fig. 6b and Table 2). Again, this was consistent with the hypothesis that soluble WT penton base competed in *trans* with Ad virions at the endocytosis stage for both nonspecific and specific secondary receptors. Mutant W119H showed a stronger competition effect than WT, with a gene delivery efficiency of 0.55 (Table 2). Several mutants, however, showed a positive effect and significantly increased the efficiency of luciferase gene delivery. The most efficient ones included the integrin-binding mutants R340E and $K^{288}E^{340}$, but K556E (1.8- to 2.2-fold), and to a lesser extent (1.2- to 1.5-fold), D288K, R340G, W439H, C551S, Y553F, and Ct550 were also efficient (Table 2). This confirmed that integrin-binding mutants as well as mutants in the C-terminal basic domain (at residues Trp439, Cys551, Tyr553, and Lys556) competed with Ad more efficiently than WT penton base for nonspecific receptor molecules, hence facilitating virion interaction with true receptors, leading to productive infection.

DISCUSSION

The aim of the present study was to better understand the early stages of Ad infection by identifying the peptide sequences specifically involved in the interaction of Ad capsid components with host cell partner proteins during Ad attachment at the cell surface and subsequent endocytosis. Besides the fiber, penton base plays a crucial role in virus-cell interactions. Biological functions associated with Ad2 penton base were thus investigated by mutagenesis of recombinant penton base protein and characterization of the mutants isolated from baculovirus-infected cells. The effects of the mutations were

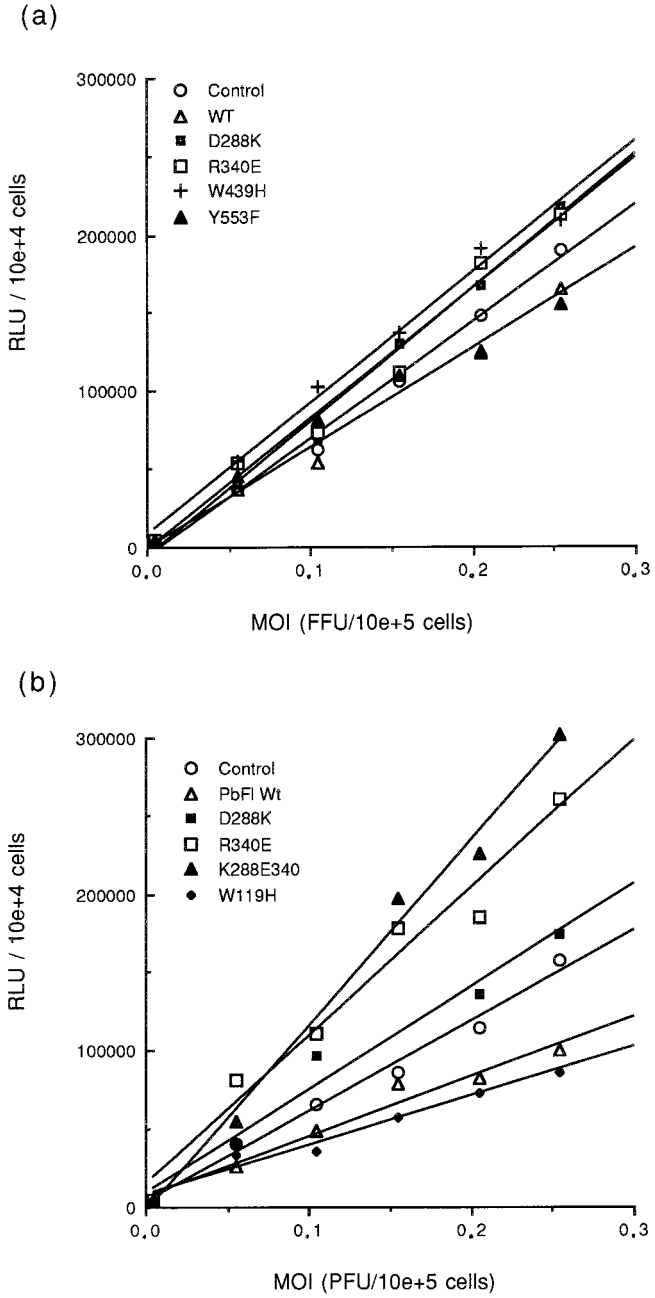

FIG. 6. Dose response of luciferase activity, expressed as RLU, in HeLa cells infected with Ad5Luc3 at varying MOI in the absence (control) or presence of constant amounts of penton base, WT, or mutants added in *trans*. (a) Cell attachment. Ad5Luc3 and penton base were incubated with cell monolayers at 0°C for 1 h, unadsorbed virus was rinsed off, and cells were harvested after further incubation at 37°C for 18 h. (b) Endocytosis. Ad5Luc3 was preincubated with cell monolayers at 0°C for 1 h, unadsorbed virus was removed, and penton base was added at the time of temperature shift to 37°C. Cells were further incubated for 18 h and processed for luciferase assays. Values represent the averages of three separate assays.

analyzed in *cis* in both Sf9 and HeLa cells (Table 1) and in *trans* in infection of HeLa cells with Ad virions (WT, Ad5, or Ad5Luc3 recombinant) in the presence of penton base proteins, WT, or mutants (Table 2).

With respect to Ad structure, assembly, and physiology, we found that any of the three substitutions W119H, Y553F, or K556E or substitutions in the polybasic ^{547}RRR at the C terminus was sufficient to abolish penton base pentamerization. Pentamer formation was also debilitated in mutants R254E, W422H, C432S, and W439H. The polybasic motif ^{547}RRR was only partially involved in the nuclear addressing of penton base in Sf9 cells, whereas substitutions W119H and W165H almost completely abolished its nuclear localization. There was no direct correlation between nuclear localization and penton base pentamerization. For example, mutant W165H, which occurred in pentameric form, accumulated within the cytoplasm, but R340E pentamers were mainly found within the nucleus (Table 1). The nuclear accumulation of R340E suggested the existence of cytoplasmic anchoring domain(s) in penton base protein.

In coexpression experiments of penton base and fiber in Sf9 cells, assembly into penton capsomer was significantly reduced for R254E, mutated in the fiber primary binding site (24) but not completely abolished. This implied that residues other than Arg254 were involved in the formation and/or stabilization of penton capsomer. This was confirmed by the observation that mutations at positions Cys432, Trp439, and Lys556 and in the polybasic stretch ^{547}RRR were deleterious to penton formation (Fig. 3a and Table 1). The finding that some of these residues were essential for pentamerization did not necessarily imply that both processes were related, and the failure of some penton base mutants to interact with fiber to form penton capsomer was not always related to their lack of pentamerization. For example, mutants W119H and Y553F, occurring as monomers, interacted with fiber in a band shift assay (Fig. 3a). The penton capsomers obtained with these two mutants were indistinguishable by EM after negative staining from natural penton capsomers isolated from Ad2 virions or Ad2-infected human cells (data not shown). This result suggested that the fiber tail domain could participate in the stabilization of the penton base pentameric structure. This hypothesis was supported by the recent report that an oligopeptide containing the 20 N-terminal residues of the fiber tail (including the penton base binding motif NPVYPY [24]) could stabilize fiberless Ad3 dodecons (17). It was noteworthy that the integrin-binding mutant R340E assembled significantly less penton capsomer than the WT penton base (Fig. 3a and Table 1). This suggested a topological and/or functional linkage between the integrin-binding domain and the fiber-binding domain in penton base and supported the hypothesis of a mechanism of ligand exchange occurring upon penton base-integrin interaction at the cell surface (24).

Penton base and $\alpha_v\beta_3$ integrin recognition (62, 63) and cell-detaching effect have both been attributed to the RGD motifs of penton base (2, 3). The cell-detaching capacity was found to be severely debilitated for our RGD mutant R340E, as observed with RGD mutant virions (3). The phenotype of the R340E mutation for the free penton base capsomer was therefore similar to that for the virion-encapsidated mutant protein. The cell-detaching effect was also lower for D288K, a mutant in the LDV motif specific for $\alpha_4\beta_1$ and $\alpha_4\beta_7$ integrins, and for mutants C246S and W165H. This suggested that the regions including Asp288, Arg340, Cys246, and Trp165 were functionally (and possibly topologically) linked in the competition with cell adhesion motifs of extracellular matrix proteins. Furthermore, W165H showed the same cell-binding defective phenotype as integrin-binding mutants D288K, R340E, R340G, and $K^{288}E^{340}$ (Fig. 5a and b), and its defect also involved specific receptors (Fig. 5c). Penton base internalization seemed to occur with a lower efficiency for W165H and for mutants in the integrin-binding motifs RGD and LDV. This further supported the hypothesis that W165H belonged to the functional

TABLE 2. Effects of penton base mutations on Ad-cell interactions in *trans*

Mutant or control	Cell attachment[a]		Ratio of ^{3}H-labeled Ad5/Ad5Luc3 attachment	Endocytosis[b]		Ratio of ^{3}H-labeled Ad5/Ad5Luc3 endocytosis
	^{3}H-labeled Ad5	Ad5Luc3		^{3}H-labeled Ad5	Ad5Luc3	
Control	100	100	1.00	100	100	1.00
FL571WT	104	88	0.88	92	69	0.75
C246S	68	125	1.84	98	100	1.02
C426S	69	94	1.36	90	78	0.86
C432S	82	113	1.37	89	98	1.10
C551S	107	90	0.84	96	145	1.51
W119H	86	102	1.18	105	58	0.55
W165H	99	120	1.21	137	112	0.82
W406H	106	113	1.06	128	119	0.93
W422H	82	99	1.20	88	70	0.79
W439H	69	135	1.95	95	137	1.44
D288K	70	133	1.90	100	122	1.22
R340E	80	127	1.59	90	170	1.89
R340G	88	96	1.09	89	107	1.20
$K^{288}R^{340}$	93	94	1.01	94	205	2.18
R254E	106	96	0.90	78	84	1.08
$RRR^{547}EQQ$	94	103	1.09	86	100	1.16
Y553F	95	88	0.92	82	115	1.40
K556E	77	93	1.20	78	142	1.82
At69	114	93	0.81	89	77	0.86
Ct550	101	132	1.30	88	127	1.44
Ct531	135	147	1.08	104	91	0.87

[a] Cell attachment of [^{3}H]thymidine-labeled Ad5 or Ad5Luc3 was performed at 0°C in the absence (control) or the presence of recombinant penton base, WT, or mutant. Cell-bound radioactivity was expressed as the percentage of values in control samples. SDs were within 15% of the reported M values (n = 4). Luciferase activity, expressed as percentage of control samples, corresponded to the slopes of the regression lines presented in Fig. 6a.

[b] Endocytosis of ^{3}H-labeled Ad5 or Ad5Luc3 was carried out at 37°C in the absence (control) or the presence of recombinant penton base, WT, or mutant. Intracellular radioactivity was expressed as the percentage of values in control samples. SDs were within 15% of the reported M values (n = 4). Luciferase activity, expressed as percentage of control samples, corresponded to the slopes of the regression lines presented in Fig. 6b.

domain(s) including the integrin-binding motifs RGD and/or LDV.

Penton base facilitation of HRP internalization into HeLa cells did not seem to follow the pathway of the RGD or LDV-dependent integrins, in contrast to plasmid DNA delivery. Penton base-mediated enhancement of PEI-complexed DNA vector delivery was apparently dependent upon the integrity of the integrin-binding motifs as well as that of residues 165, 246, 422, and 439. When added in excess in *trans* to Ad on HeLa cell monolayers, integrin-binding mutants D288K and R340E, as well as W165H, C246S, and W439H, significantly enhanced the attachment of Ad to specific receptors. In endocytosis assays, R340E, the double mutant $K^{288}E^{340}$, and K556E augmented twofold the efficiency of Ad-mediated gene delivery, whereas W119H showed a negative effect, with an apparent sequestration of Ad5Luc3 within the endosomal vesicles (Table 2), suggesting a function of the Trp119 residue at the postendocytotic stage.

Thus, the overall phenotypic characterization of our penton base mutants suggested that the two integrin-binding motifs RGD^{340} and LDV^{287} and discrete regions including Trp119, Trp165, and Cys246 in the N-terminal moiety and Cys432 and Trp439 in the C-terminal moiety belonged to functional domain(s) involved in penton base-receptor interaction, endocytosis, and postendocytotic steps. Our analysis of recombinant penton base mutants was therefore a preliminary but necessary step to the understanding of molecular mechanisms of Ad cell attachment, endocytosis, vesicular escape, and nuclear addressing, all crucial and limiting steps for efficient gene therapy with adenoviral vectors. The replacement of some of our penton base mutations into the Ad genome and the isolation of Ad mutants with a particular phenotype (3) will be the next step to elucidate the successive reactions and cellular molecules that play a role in endosomal and postendosomal phases of the Ad life cycle.

ACKNOWLEDGMENTS

We are grateful to Liliane Cournud for expert secretarial aid and to Martine Bardy for help with the cell cultures.

This work was supported in part by the Association Française de Lutte contre la Mucoviscidose (AFLM grant 96-022), the Association Française contre les Myopathies (AFM grant 96-4889), and the Centre National de la Recherche Scientifique (AI-Biologie Cellulaire DSV-96 001). S.S.H. was the recipient of a fellowship from the AFLM.

REFERENCES

1. **Adam, S. A.** The importance of importin. Trends Cell Biol. **5:**189–191.
2. **Bai, M., L. Campisi, and P. Freimuth.** 1994. Vitronectin receptor antibodies inhibit infection of HeLa and A549 cells by adenovirus type 12 but not by adenovirus type 2. J. Virol. **68:**5925–5932.
3. **Bai, M., B. Harfe, and P. Freimuth.** 1993. Mutations that alter an Arg-Gly-Asp (RGD) sequence in the adenovirus type 2 penton base protein abolish its cell-rounding activity and delay virus reproduction in flat cells. J. Virol. **67:**5198–5205.
4. **Belin, M. T., and P. Boulanger.** 1993. Involvement of cellular adhesion sequences in the attachment of adenovirus to HeLa cell surface. J. Gen. Virol. **74:**1485–1497.

5. **Bergelson, J. M., J. A. Cunningham, G. Droguett, E. A. Kurt-Jones, A. Krithivas, J. S. Hong, M. S. Horwitz, R. L. Crowell, and R. W. Weinberg.** 1997. Isolation of common receptor for coxsackie B viruses and adenoviruses 2 and 5. Science **275:**1320–1323.
6. **Boudin, M. L., and P. Boulanger.** 1982. Assembly of adenovirus penton base and fiber. Virology **116:**589–604.
7. **Boudin, M. L., M. Moncany, J. C. D'Halluin, and P. Boulanger.** 1979. Isolation and characterization of adenovirus type 2 vertex capsomer (penton base). Virology **92:**125–138.
8. **Boudin, M. L., J. C. D'Halluin, C. Cousin, and P. Boulanger.** 1980. Human adenovirus type 2 protein IIIa. II. Maturation and encapsidation. Virology **101:**144–156.
9. **Boussif, O., F. Lezoualc'h, M. A. Zanta, M. D. Mergny, D. Scherman, B. Demenex, and J.-P. Behr.** 1995. A versatile vector for gene and oligonucleotide transfer into cells in culture and in vivo: polyethylenimine. Proc. Natl. Acad. Sci. USA **92:**7297–7301.
10. **Carrière, C., B. Gay, N. Chazal, N. Morin, and P. Boulanger.** 1995. Sequence requirements for encapsidation of deletion mutants and chimeras of human immunodeficiency virus type 1 Gag precursor into retrovirus-like particles. J. Virol. **69:**2366–2377.
11. **Chroboczek, J., R. W. H. Ruigrok, and S. Cusack.** 1995. Adenovirus fiber. Curr. Top. Microbiol. Immunol. **199:**165–200.
12. **Curiel, D. T., S. Agarwal, E. Wagner, and M. Cotten.** 1991. Adenovirus enhancement of transferrin-polylysine-mediated gene delivery. Proc. Natl. Acad. Sci. USA **88:**8850–8854.
13. **Cuzange, A., J. Chroboczek, and B. Jacrot.** 1994. The penton base of human adenovirus type 3 has the RGD motif. Gene **146:**257–259.
14. **Davies, D. R., and E. A. Padlan.** 1990. Antibody-antigen complexes. Annu. Rev. Biochem. **59:**439–473.
15. **Defer, C., M. T. Belin, M. L. Caillet-Boudin, and P. Boulanger.** 1990. Human adenovirus-host cell interactions: a comparative study with members of subgroups B and C. J. Virol. **64:**3661–3673.
16. **D'Halluin, J. C., C. Cousin, and P. Boulanger.** 1982. Physical mapping of adenovirus type 2 temperature-sensitive mutations by restriction endonuclease analysis of interserotypic recombinants. J. Virol. **41:**401–413.
17. **Fender, P., R. W. H. Ruigrok, E. Gout, S. Buffet, and J. Chroboczek.** 1997. Adenovirus dodecahedron, a new vector for human gene therapy. Nat. Biotechnol. **15:**52–56.
18. **FitzGerald, D. J. P., R. Padmanabhan, I. Pastan, and M. C. Willigham.** 1983. Adenovirus-induced release of epidermal growth factor and *Pseudomonas* toxin into the cytosol of KB cells during receptor-mediated endocytosis. Cell **32:**607–617.
19. **Ginsberg, H. S.** 1979. Adenovirus structural proteins, p. 409–457. *In* H. Fraenkel-Conrat and R. R. Wagner (ed.), Comprehensive virology. Plenum Press, New York, N.Y.
20. **Ginsberg, H. S., and C. S. H. Young.** 1977. Genetics of adenovirus, p. 27–88. *In* Comprehensive virology, vol. 9. Plenum Press, New York, N.Y.
21. **Görlich, D., and I. W. Mattaj.** 1996. Nucleocytoplasmic transport. Science **271:**1513–1518.
22. **Greber, U. F., M. Willetts, P. Webster, and A. Helenius.** 1993. Stepwise dismantling of adenovirus 2 entry into cells. Cell **75:**477–486.
23. **Higuchi, R., B. Krummel, and R. K. Saiki.** 1988. A general method of in vitro preparation and specific mutagenesis of DNA fragments: study of protein and DNA interactions. Nucleic Acids Res. **16:**7351–7367.
24. **Hong, S. S., and P. Boulanger.** 1995. Protein ligands of the human adenovirus type 2 outer capsid identified by biopanning of a phage-displayed peptide library on separate domains of wild-type and mutant penton capsomers. EMBO J. **14:**4714–4727.
25. **Hong, S. S., L. Karayan, J. Tournier, D. T. Curiel, and P. Boulanger.** 1997. Adenovirus type 5 fiber knob binds to the MHC class I alpha-2 domain at the surface of human epithelial and B lymphoblastoid cells. EMBO J. **16:**2294–2306.
26. **Huang, S., T. Kamata, Y. Takada, Z. M. Ruggeri, and G. R. Nemerow.** 1996. Adenovirus interaction with distinct integrins mediates separate events in cell entry and gene delivery to hematopoietic cells. J. Virol. **70:**4502–4508.
27. **Humphries, M. J.** 1990. The molecular basis and specificity of integrin-ligand interactions. J. Cell Sci. **97:**585–592.
28. **Karayan, L., B. Gay, J. Gerfaux, and P. Boulanger.** 1994. Oligomerization of recombinant penton base of adenovirus type 2 and its assembly with fiber in baculovirus-infected cells. Virology **202:**782–796.
29. **Komoryia, A., L. J. Green, M. Mervic, S. S. Yamada, K. M. Yamada, and M. J. Humphries.** 1991. The minimal essential sequence for a major cell type-specific adhesion site (CS-1) within the alternatively spliced type III connecting segment domain of fibronectin is leucine-aspartic acid-valine. J. Biol. Chem. **266:**15075–15079.
30. **Kunkel, T. A., J. D. Roberts, and R. A. Zakour.** 1987. Rapid and efficient site-specific mutagenesis without phenotypic selection. Methods Enzymol. **154:**367–383.
31. **Lonberg-Holm, K., and L. Philipson.** 1969. Early events of virus-cell interaction in an adenovirus system. J. Virol. **4:**323–338.
32. **Luckow, V. A., and M. D. Summers.** 1989. High level expression of nonfused foreign genes with *Autographa californica* nuclear polyhedrosis virus expression vectors. Virology **170:**31–39.
33. **Martin, G. R., R. Warocquier, C. Cousin, J. C. D'Halluin, and P. Boulanger.** 1978. Isolation and phenotypic characterization of human adenovirus type 2 temperature-sensitive mutants. J. Gen. Virol. **41:**303–314.
34. **Mathias, P., T. Wickham, M. Moore, and G. R. Nemerow.** 1994. Multiple adenovirus serotypes use α_V integrins for infection. J. Virol. **68:**6811–6814.
35. **Mittal, S. K., M. R. McDermott, D. C. Johnson, L. Prevec, and F. L. Graham.** 1993. Monitoring foreign gene expression by a human adenovirus-based vector using the firefly luciferase gene as a reporter. Virus Res. **28:**67–90.
36. **Neer, E. J., C. J. Schmidt, R. Nambudripad, and T. F. Smith.** 1994. The ancient regulatory-protein family of WD-repeat proteins. Nature (London) **371:**297–300.
37. **Nemerow, G. R., D. A. Cheresh, and T. J. Wickham.** 1994. Adenovirus entry into host cells: a role for α_v integrins. Trends Cell Biol. **4:**52–55.
38. **Nermut, M. V.** 1984. The architecture of adenoviruses, p. 5–34. *In* H. S. Ginsberg (ed.), The adenoviruses. Plenum Publishing Corp., New York, N.Y.
39. **Neumann, R., J. Chroboczek, and B. Jacrot.** 1988. Determination of the nucleotide sequence for the penton base gene of human adenovirus type 5. Gene **69:**153–157.
40. **Novelli, A., and P. Boulanger.** 1991. Deletion analysis of functional domains in baculovirus-expressed adenovirus type 2 fiber. Virology **185:**365–376.
41. **Otero, N. J., and L. Carrasco.** 1987. Proteins are co-internalized with virion particles during early infection. Virology **160:**75–80.
42. **Persson, R., U. Svensson, and E. Everitt.** 1985. Virus receptor interaction in the adenovirus system: characterization of the positive cooperative binding of virions on HeLa cells. J. Virol. **54:**92–97.
43. **Pettersson, U.** 1984. Structural and non-structural adenovirus proteins, p. 205–270. *In* H. S. Ginsberg (ed.), The adenoviruses. Plenum Publishing Corp., New York, N.Y.
44. **Philipson, L., K. Lonberg-Holm, and U. Pettersson.** 1968. Virus-receptor interaction in an adenovirus system. J. Virol. **2:**1064–1075.
45. **Roberts, R. J., G. Akusjärvi, P. Aleström, R. E. Gelinas, T. R. Gingeras, D. Sciaky, and U. Pettersson.** 1986. A consensus sequence for the adenovirus 2 genome, p. 1–51. *In* W. Doerfler (ed.), Adenovirus DNA: the viral genome and its expression. Martinus Nijhoff, Boston, Mass.
46. **Ruigrok, R. W. H., A. Barge, C. Albiges-Rizo, and S. Dayan.** 1990. Structure of adenovirus fibre. II. Morphology of single fibres. J. Mol. Biol. **215:**589–596.
47. **Russel, M., S. Kidd, and M. R. Kelley.** 1986. An improved filamentous helper phage for generating single-stranded plasmid DNA. Gene **45:**333–338.
48. **Sanger, F., S. Nicklen, and A. R. Coulson.** 1977. DNA sequencing with chain terminating inhibitors. Proc. Natl. Acad. Sci. USA **74:**5463–5467.
49. **Seth, P.** 1994. Adenovirus-dependent release of choline from plasma membrane vesicles at an acidic pH is mediated by the penton base protein. J. Virol. **68:**1204–1206.
50. **Seth, P., D. FitzGerald, H. S. Ginsberg, M. Willingham, and I. Pastan.** 1984. Evidence that the penton base of adenovirus is involved in potentiation of toxicity of *Pseudomonas* exotoxin conjugated to epidermal growth factor. Mol. Cell. Biol. **4:**1528–1533.
51. **Seth, P., M. Rosenfeld, J. Higginbotham, and R. G. Crystal.** 1994. Mechanism of enhancement of DNA expression consequent to cointernalization of a replication-deficient adenovirus and unmodified plasmid DNA. J. Virol. **68:**933–940.
52. **Sheppard, M., and H. Trist.** 1992. Characterization of the avian adenovirus penton base. Virology **188:**881–886.
53. **Stewart, P. L., R. M. Burnett, M. Cyrklaff, and S. D. Fuller.** 1991. Image reconstruction reveals the complex molecular organization of adenovirus. Cell **67:**145–154.
54. **Stouten, P. F. W., C. Sader, R. W. H. Ruigrok, and S. Cusack.** 1992. New triple-helical model for the shaft of the adenovirus fibre. J. Mol. Biol. **226:** 1073–1084.
55. **Svensson, U.** 1985. Role of vesicles during adenovirus 2 internalization into HeLa cells. J. Virol. **55:**442–449.
56. **Svensson, U., and R. Persson.** 1984. Entry of adenovirus 2 into HeLa cells. J. Virol. **51:**687–694.
57. **Tomko, R. P., R. Xu, and L. Philipson.** HCAR and MCAR: the human and mouse cellular receptors for subgroup C adenoviruses and group B coxsackieviruses. 1997. Proc. Natl. Acad. Sci. USA **94:**3352–3356.
58. **van Oostrum, J., and R. M. Burnett.** 1985. Molecular composition of the adenovirus type 2 virion. J. Virol. **56:**439–448.
59. **Varga, M. J., C. Weibull, and E. Everitt.** 1991. Infectious entry pathway of adenovirus type 2. J. Virol. **65:**6061–6070.
60. **White, J. M.** 1993. Integrins as virus receptors. Curr. Biol. **3:**596–599.
61. **Wickham, T. J., M. E. Carrion, and I. Kovesdi.** 1995. Targeting of adenovirus penton base to new receptors through replacement of its RGD motif with other receptor-specific peptide motifs. Gene Ther. **2:**750–758.
62. **Wickham, T. J., E. J. Filardo, D. A. Cheresh, and G. R. Nemerow.** 1994. Integrin $\alpha_v\beta_5$ selectively promotes adenovirus-mediated cell membrane permeabilization. J. Cell Biol. **127:**257–264.

63. **Wickham, T. J., P. Mathias, D. A. Cheresh, and G. R. Nemerow.** 1993. Integrins $\alpha_v\beta_3$ and $\alpha_v\beta_5$ promote adenovirus internalization but not virus attachment. Cell **73:**309–320.
64. **Wickham, T. J., D. M. Segal, P. W. Roelvink, M. E. Carrion, A. Lizonova, G. M. Lee, and I. Kovesdi.** 1996. Targeted adenovirus gene transfer to endothelial and smooth muscle cells by using bispecific antibodies. J. Virol. **70:**6831–6838.
65. **Wohlfart, C.** 1988. Neutralization of adenoviruses: kinetics, stoichiometry, and mechanisms. J. Virol. **62:**2321–2328.
66. **Yamada, K. M.** 1989. Fibronectins: structure, functions and receptors. Curr. Opin. Cell Biol. **1:**956–963.
67. **Yoshimura, A.** 1985. Adenovirus-induced leakage of co-endocytosed macromolecules into the cytosol. Cell Struct. Funct. **10:**391–404.
68. **Yoshimura, K., M. A. Rosenfeld, P. Seth, and R. G. Crystal.** 1993. Adenovirus-mediated augmentation of cell transformation with unmodified plasmid vectors. J. Biol. Chem. **268:**2300–2303.